Groundwater Monitoring&Remediation

Vadose Zone Soil Flushing for Chromium Remediation: A Laboratory Investigation to Support Field-scale Application

by James E. Szecsody, Hilary P. Emerson, Amanda R. Lawter, Charles T. Resch, Mark L. Rockhold, Rob D. Mackley and Nikolla P. Qafoku

Abstract

Cr(VI) flushing from the vadose zone to the groundwater (with subsequent Cr(VI) removal in groundwater by pump-and-treat system) is a promising remedial technique that has recently been used at field scale. This laboratory study was conducted to provide the technical basis to design a field soil flushing strategy. The objectives were to (1) quantify the relationship between sediment Cr(VI) and Cr(III) mass and release rates and subsequent Cr(VI) leaching; (2) investigate different methodologies to maximize Cr(VI) leaching, and (3) investigate methods to minimize leaching of remaining residual Cr. Characterization of Cr-contaminated sediments (Hanford Site, WA) exhibited Cr(VI) showed that leach rates that were correlated to different Cr surface phases. Sediments with low leachable Cr(VI) (<2 μg/g) leached Cr rapidly, so slow infiltration of water in a single pulse was sufficient to leach most Cr. In contrast, sediments with high Cr (2 to 200 μg/g) released some Cr(VI) quickly but 10 to 50% Cr(VI) slowly (tens to hundreds of hours). Efficient unsaturated leaching of these sediments required a different infiltration strategy that includes: multiple slow leach pulses with time between flushing cycles; the use of a surfactant to increase Cr leaching from low-permeability zones, and the use of a reductant (Na-dithionite or Ca-polysulfide) in the final leach water was highly effective at decreasing residual Cr leaching. This study clearly demonstrated that the methodology of basing laboratory Cr flushing on parameters such as Cr release mass and rates could be used to improve the efficiency of soil flushing at field scale.

Introduction

Despite many efforts over the last few decades to remediate hexavalent chromium (Cr(VI)) contaminated sites around the world (Jacobs and Testa 2005), Cr(VI) contamination persists in many soils, subsoils, and sediments (Szecsody et al. 2019; Rockhold et al. 2020). This is a major concern because the oxidized hexavalent form, Cr(VI), has a higher toxicity than the reduced, mostly immobile, trivalent form, Cr(III). Many in situ remediation technologies have been developed and applied in Cr(VI)-contaminated groundwater sites, such as the use of permeable reactive (reductive) barriers (Wilkin et al. 2005), application(s) of strong abiotic reductants to reduce and remove Cr(VI) from solution via precipitation (Vermeul et al. 2004; Dresel et al. 2008; Zhong et al. 2009), bioreduction, phytoremediation (Shams et al. 2010; Zheng et al. 2020), and natural attenuation (Last et al. 2015; Truex et al. 2015). However, remediation of Cr-contaminated sites remains challenging mainly because of the heterogeneity of subsurface Cr contamination; the occurrence of a variety of Cr-containing phases that exhibit difficult-to-predict geochemical behavior; the presence of other redox-sensitive co-contaminants as part of a complex contaminant mixture; and the existence of hard-to-access subsurface locations, or concentrated vadose zone Cr hot spots, that serve as a continuous source of groundwater (GW) contamination.

The Hanford Site, a former nuclear-materials production site in southeastern Washington State (United States), has multiple Cr GW plumes due to releases decades ago from historical corrosion inhibition use in nuclear reactors.

Article impact statement: Field scale Cr soil flushing can be efficiently designed based on characterization of sediment Cr surface phases, release rate, and field scale heterogeneities.

doi: 10.1111/gwmr.12570

Cr contamination persists in the vadose zone due to geochemical and physical processes. The majority of Cr at the site was released as aqueous chromate (CrO_4^{2-}) that exhibits nearly no adsorption to sediments under neutral and slightly alkaline conditions (Zachara et al. 1989, 2004; Qafoku et al. 2009; Szecsody et al. 2019) or near-surface releases of acidic, high-concentration sodium dichromate ($Na_2Cr_2O_7$). Considerable chromate adsorption and partial reduction has been observed under acidic conditions (Stanin 2005; Dresel et al. 2008; Qafoku et al. 2010). As the acid is neutralized by reactions with sediments (carbonates and clay minerals; Szecsody et al. 2013), chromate either precipitates with calcium (Ca) or barium (Ba) (Palmer and Willbrodt 1991; Arcon et al. 2005), coprecipitates with calcium carbonate ($CaCO_3$) (Robles-Camacho and Armienta 2000; Tang et al. 2007), or adsorbs to manganese (Mn), aluminum (Al), and iron (Fe) oxides and clay minerals (Zachara et al. 1987; Rai et al. 1989; Vermeul et al. 2004).

Significant aqueous Cr removal has been also reported when highly basic saline waste fluids interact with the sediments (Qafoku et al. 2003). The mineral dissolution that occurs under either acidic or alkaline conditions may have triggered the release of Fe(II) from the Fe(II)-bearing minerals, which subsequently reduces aqueous Cr(VI) (Qafoku et al. 2003, 2010, 2011). Other studies have shown that under acidic conditions, Fe(II) in phyllosilicates (Szecsody et al. 2013) and Fe oxides (Dong et al. 2003) can also reduce aqueous Cr(VI). These previous studies provide evidence for Cr contamination persistence, and for large differences in released Cr mass from different sediments, mainly because of the contributions of multiple Cr(VI)-bearing solids. The existence of multiple forms of Cr(VI), that is, aqueous, adsorbed, and coprecipitated, makes the remediation of Cr-contaminated sites challenging. A continued source of Cr from the vadose zone is inferred from GW sampling data, which show persistent Cr in GW and increasing Cr following periods of an elevated water table.

Worldwide, Cr remediation is achieved by excavation of contaminated sediments, pump-and-treat (P&T) in GW (Jacobs and Testa 2005), in situ abiotic and biotic reductive barriers in GW (Vermeul et al. 2002; Brodie et al. 2011), reductive gas injection in the vadose zone (Thornton et al. 2007), and soil flushing in the vadose zone coupled with GW P&T (DOE/RL-2019-77 2020). Soil flushing is a technology that has the potential to remove Cr from contaminated vadose zone sediments (DOE-RL-2021-31 2020; Szecsody et al. 2021). Soil flushing consists of percolating excess water in the vadose zone at a specific rate in one or more pulses, and if needed, adding appropriate mobilizing agents to increase Cr mobility so that it can be flushed downward into the GW system. Once the Cr is in GW, it can be hydraulically captured and subsequently removed with a P&T system. At the Hanford Site, soil flushing and GW P&T operations rely on Cr leaching from the vadose zone to change Cr concentrations in GW. Increased effectiveness of soil flushing activities will likely be achieved by designing field-based operations based on an improved technical understanding of the key geochemical and physical factors controlling removal of residual Cr(VI) from the aqueous, adsorbed, and solid phases in sediments as well as tracking the wetting front advance during soil flushing. Even in homogeneous sediments, infiltration of water occurs primarily through larger advective pores, and Cr trapped in smaller diffusive pores, which usually occur next to smaller grains, migrates more slowly due to decreased flow. In heterogeneous vadose zone sediments, low-permeability zones that typically have a higher water content and greater aqueous Cr are more difficult to flush, as capillary forces tend to limit water migration through the lenses and cause infiltrating water to flow around low-permeability lenses. Efficient soil flushing of Cr from the vadose zone requires that (1) Cr leach mass and rate from sediments is known in order to optimize the infiltration rate and duration and (2) field scale heterogeneities (i.e., low permeability zones with trapped Cr) are characterized such that efficiency of increasing Cr leaching using surfactant amendments to increase water flow through these zones can be evaluated.

To understand key geochemical and physical processes controlling Cr movement in vadose zone sediments, the objectives of this work were to (1) quantify sediment Cr mass, release rates, and surface phase changes as Cr is leached out from different sediments; (2) evaluate different leach solutions and strategies to maximize the amount of Cr leached and minimize the time required for soil flushing; and (3) investigate methods to minimize leaching of residual Cr after soil flushing ends. To achieve these objectives, we conducted a laboratory study using contaminated sediments (including an artificial sediment with multiple Cr surface phases) that exhibited a wide variety of Cr(VI) leach behavior (e.g., fast vs. slow, different phases, different concentrations). We performed chemical extractions of different strengths, and a series of water-saturated and unsaturated column experiments that used GW, GW mixed with cationic and anionic surfactants to enhance Cr leaching during flushing, or reductants (Na-dithionite, Ca-polysulfide) to decrease Cr leaching after soil flushing ends. Because some Cr may be trapped in low-permeability zones present in the field, two-dimensional (2D) infiltration experiments were conducted to quantify the extent to which a cationic or anionic surfactant addition to the infiltration water increases water flow into and through low-permeability zones. The surfactant reduces the surface tension of the infiltrating water, resulting in more rapid infiltration through inclusions. At field scale, low-permeability inclusions are likely to have higher water content, and therefore may contain greater aqueous and adsorbed Cr. These finer-grained inclusions also have higher surface area, so they may also contain higher concentrations of Cr in precipitates. In addition, different infiltration strategies were evaluated that included different infiltration rates and multiple infiltration pulses. The effects of these geochemical and physical processes on Cr leaching were used to develop a technical framework and understanding that could support highly efficient field-scale soil flushing. Field-scale soil leaching has been conducted in two Hanford Site areas and is being considered for other Cr-contaminated areas (DOE/RL-2019-77 2020; SWG-67175 2021; DOE/RL-2021-31 2022). The methodology developed and described in this study is also applicable to many other Cr-contaminated sites around the globe.

Materials and Methods

Characteristics of the field-contaminated and synthetic Hanford sediments used to evaluate chromate leaching behavior are provided in "Sediments" section. "Sequential extractions targeting total Cr and Cr(VI)" section describes the sequential extractions used to quantify Cr mass and surface phase changes as Cr is leached from different Hanford sediments. Column experiments conducted for evaluation of Cr leach rate, effect of different leach solutions, and leach strategies to maximize Cr leaching during soil flushing and minimize leaching of remaining residual Cr after soil flushing ends are described in "Column experiments" section, with details on liquid phase analyses in "Extraction and leach sample analyses" section. A description of the modeling used to quantify the Cr release rate and mass from the unsaturated leach experiments is provided in "Simulation of 1D infiltration experiments" section.

Sediments

Four representative Cr-contaminated sediments used in this study were collected from the 100-D Area vadose zone (R5, R28), 100-D Area saturated zone (R8), and 200 East Area vadose zone (R25) at the Hanford Site (Table 1). Additional sediments from Hanford Site borehole samples were subjected to a broader investigation (Szecsody et al. 2022). Previous Cr characterization of the sediments, when available, was compared to sequential extractions and leaching conducted in this study. Previous leach and sequential extractions studies (of sediments from the Hanford 100 Area) generally showed that only a small portion of natural Cr in uncontaminated Hanford sediments was leachable and was Cr(VI) whereas the majority of natural Cr in sediments was Cr(III), as confirmed by ion chromatography separation of Cr phases and inductively coupled plasma-mass spectrometry (ICP-MS, Szecsody et al. 2020a). In addition, X-ray adsorption near edge structure analysis of a Hanford sediment with low Cr contamination showed mostly Cr(III) consistent with Cr in Fe oxides, with a small fraction of Cr(VI), consistent with $CaCrO_4$ and chromate-substituted calcite (Szecsody et al. 2020b). In contrast, sediments with high Cr contamination had a higher fraction of leachable Cr, which implied that a larger fraction the anthropogenic Cr was Cr(VI). For the 100-K area sediment.

In addition to field-contaminated sediments, a synthetic sediment was made with multiple Cr precipitates to evaluate Cr leaching rate from the different phases. This synthetic sediment (R30, Table 1); consisted of about 40% gravel and 60% less than 2-mm material with natural chromium in the sediment totaled 11.62 µg/g, with 0.013 µg/g leachable Cr. Cr was then added to the sediment in multiple Cr phases, including $BaCrO_4$ (Alfa Aesar; 14.43 µg/g Cr, considered low leaching rate), $CaCrO_4$ (Alfa Aesar; 4.79 µg/g Cr, considered to have a high leaching rate), and laboratory-produced Cr-substituted calcite (0.42 µg/g Cr, considered to have a slow leaching rate), for a total of 31.26 µg/g Cr, with 19.5 µg/g labile Cr. Sequential extractions were also conducted on $CaCrO_4$ alone (82 mg), which should yield a total of 27.3 mg/g Cr.

Table 1

Cr-contaminated Sediments Used in This Study

No.	Area	Borehole/Depth	Location
R28	100-D	100-D-104, 20′, drain of 183-D yellow YS, YS2	Vadose zone
R8	100-D	C8954 83.4′	Saturated
R25	200 VZ S-13	C9513 131.5′	Vadose zone
R5	100-D	C8953 82′	Saturated
R30		Artificial sediment, multiple Cr phases	

Sequential Extractions Targeting Total Cr and Cr(VI)

Sequential liquid extractions have been used to evaluate the aqueous, adsorbed, and solid precipitates for metals including uranium (U), Ca, Cr, copper (Cu), phosphorous (P), Fe, Mn, Al, and silicon (Si) (Chao and Zhou 1983; Hall et al. 1996; Gleyzes et al. 2002; Sutherland and Tack 2002; Mossop and Davison 2003; Larner et al. 2006). Sequential extractions were used to determine the aqueous, adsorbed, and precipitated Cr phases in the untreated and postleach sediments. Concentrations of other elements were also measured in some extractions, including Ca, magnesium (Mg), and Ba, which form Cr-bearing solid phases such as Cr-substituted carbonates and Ba-chromate. Some sediments had a total Cr concentration below the detection limit of X-ray diffraction (~0.5% of each mineral), so sequential liquid extractions were used to operationally determine Cr phases before and after leaching.

Six increasingly acidic sequential extractions were used in this investigation that included: (1) artificial groundwater (AGW), (2) ion exchange solution, (3) pH 5 acetate solution, (4) pH 2.3 acetic acid, (5) oxalic acid, and (6) nitric acid, where target Cr phases are described in Table 2 (Szecsody et al. 2019). Extraction 3 (pH 5 acetate solution) is operationally defined as the carbonate that dissolves in a weak acetate solution (pH 5) in 1 h in contrast to the 5-day acetic acid extraction (extraction 4, pH 2.3), which dissolves most carbonates in the 5-day extraction. Anthropogenic contaminants that incorporate into calcite can be preferentially incorporated in a thin rind on the calcite surface. In this study, "labile Cr" is defined as the the Cr in extractions 1, 2, and 3. Extractions used pre- or postleach sediment (3 to 5 g) and solution (6 to 10 mL) placed in 45-mL polytetrafluoroethylene (PTFE) centrifuge tubes. Extraction 1 consisted of mixing the sediment with AGW (1:2 sediment: water ratio in a 45-mL PTFE tube) for 1.0 h at 25 °C. The chemical composition of AGW is provided in Table S1 (Supporting information). The tubes were then centrifuged at 3000 rpm for 10 min, and the liquid was drawn off the top of the sediment and filtered (0.45-µm nylon/polyvinylidene fluoride [PVDF]) for analysis. The same protocol was used for the second, third, fourth, and fifth extractions. The sixth extraction used a 0.45-µm PTFE or PVDF filter, as the nylon filter is not compatible with strong acid.

Column Experiments

Twenty-one column experiments (6 hydraulically saturated and 15 hydraulically unsaturated experiments) were conducted to measure the extent and rates of Cr desorption from sediments under hydraulically saturated or unsaturated

Table 2

Sequential Extraction Solutions

Extraction No.	Solution	Time and Temperature	Extraction Phases
1	Artificial groundwater	1 h at 25°C	Aqueous Cr
2	0.5 mol/L $Mg(NO_3)_2$	1 h at 25°C	Adsorbed Cr
3	0.5 mol/L Na-acetate (pH 5)	1 h at 25°C	Rind-carbonate Cr
4	0.44 mol/L acetic acid, 0.20 mol/L $Ca(NO_3)_2$ (pH 2.3)	5 days at 25°C	Total carbonate Cr
5	0.1 mol/L ammonium oxalate, 0.1 mol/L oxalic acid	1 h at 25°C	Fe-oxide Cr
6	8 mol/L HNO_3	3 h at 95°C	Hard-to-extract Cr

conditions. Although soil flushing at field scale is mainly under unsaturated conditions, low-permeability zones can create water-saturated flow conditions. In addition, water-saturated columns are conducted with stop-flow (SF) events that enable calculation of Cr release rate at different times during leaching. Therefore, water-saturated leaching was used as a baseline for Cr leached mass and Cr release rate for comparison to unsaturated leach experiments. Cr leaching mass was first evaluated in one-dimensional (1D) hydraulically saturated columns leached with AGW. Unsaturated column experiments (2.9 m high) were then used to study the effect of water saturation on Cr release. Both hydraulically saturated and unsaturated experiments with AGW were used as a baseline for comparison of Cr leaching behavior with different amendments to AGW. Finally, 2D column experiments were conducted to evaluate the use of (1) surfactants to decrease the surface tension of water, which increase water flow through low-permeability lenses, and increase Cr desorption; and (2) reductants, which decrease the mobility of the residual Cr after Cr flushing is complete.

Table 3

Solutions that were Used in Hydraulically Saturated and Unsaturated Experiments

Solution No.	Solution Composition	Experiments
1	Artificial groundwater, pH 8 (Table S1)	Saturated and unsaturated
2	Artificial groundwater, pH 6 equilibrated	Saturated only
3	Artificial groundwater, pH 5 equilibrated	Saturated only
4	Reductant: AGW + 0.03 M Na-dithionite, pH 12	Saturated and unsaturated
5	Reductant: AGW + 0.03 mol/L Ca-polysulfide	Unsaturated only
6	Anionic surfactant: AGW + 500 ppm Na lauryl sulfate	Saturated and unsaturated
7	Cationic surfactant: AGW + 500 ppm benzalkonium-Cl	Unsaturated only

1D Hydraulically Saturated Column Experiments

Small water-saturated column experiments (1.6 cm diameter by 20 cm length) were used to determine total Cr leaching mass of the sediment and the rate of Cr release. Although these are saturated flow experiments, they still provide pore volumes (PVs) to leach a specific fraction of Cr mass, Cr release rates at different PVs (i.e., at SF events), and a baseline for comparison to unsaturated leach experiments. AGW or other amendments were injected into the column at a constant flow rate to achieve a 2-h residence time for a total of 7.7 to 12 PVs. The residence time is defined as the time it takes for 1 PV of water to travel through the column. Effluent samples (i.e., 30 samples for each experiment) were collected automatically in 5-mL falcon tubes using a fraction collector (Isco Foxy 200). Because Cr typically leaches from the sediment at a high initial rate, which decreases over time, more effluent samples were collected in the first two PVs than in subsequent PVs. Some experiments also included the injection of 80 mg/L bromide (Br^-), added as sodium bromide (NaBr), that behaves as a conservative (nonreactive) tracer. Other amendment solutions which were used to change Cr leaching rate included (1) weak acidic solutions (pH reduced to 6.0 and 5.0 with nitric acid); (2) cationic (benzalkonium-chloride) or anionic (Na lauryl sulfate) surfactant solutions; and (3) reductant solutions (Na-dithionite and Ca-polysulfide) (Table 3). The weak acidic solutions consisted of AGW that was equilibrated to pH = 6.0 over several days using a small addition of nitric acid (HNO_3). The surfactant solution consisted of 500 mg/L of an anionic surfactant, Na lauryl sulfate (CAS 151-21-3, $CH_3(CH_2)11(OCH_2CH_2)_nOSO_3Na$), or 500 mg/L of a cationic surfactant, benzalkonium chloride (CAS 63499-41-2, $C_6H_5CH_2N(CH_3)_2RCl$ [$R = C_8H_{17}$ to $C_{18}H_{37}$]). The first reductant solution was 0.03 mol/L Na-dithionite and 0.12 mol/L K_2CO_3 (pH = 12) and was injected initially from 1.0 to 2.5 PVs ("part reductant") or over all PVs ("full reductant"). The second reductant solution was a Ca polysulfide solution (0.3 mol/L) over all PVs. The conditions for the column experiments are summarized in Table 4. Although there were no direct duplicate water-saturated experiments, pH 6 and pH 8 AGW experiments showed little difference, so the standard deviation of the leached Cr between pairs for sediments R5 and R25 was 12%.

SF events provided time for Cr to be released from slow desorption sites, dissolving phases, and/or diffusion-controlled pores within the sediment matrix. The SF events lasted for about 16 h (at 1 PV), 150 h (at 2.5 PVs), and 500 h (at 10 to 50 PVs). A relatively short SF event (i.e., 16 h after the start) was applied at the beginning of these experiments because aqueous and adsorbed Cr are usually rapidly leached (with the first PV). Later during leaching,

Table 4

Hydraulically Saturated and 1D/2D Unsaturated Cr Leach Experiments

Sediment	Experiment No.	Experiment Type	Injection Solution	Initial v[1] (cm/h)	Final v[2] (cm/h)
R28	S18	Saturated	pH 8 AGW	5.19	
	J4	Unsaturated	pH 8 AGW	10.05	0.0401
	J6	Unsaturated	pH 8 AGW	47.4	0.00751
	J7	Unsaturated	pH 8 AGW	5.26	0.0287
	J8	Unsaturated	pH 8 AGW	16.5	0.0245
	J9	Unsaturated	Full reductant[4] (Na-dith)	55.8	0.00176
	J10	Unsaturated	Anionic surfactant	38.7	0.0043
R25	S11	Saturated	pH 8 AGW	4.61	
	S16	Saturated	pH 6 AGW	4.4	
	S17	Saturated	Part reductant[3] (Na-dith)	4.62	
	J5	Unsaturated	pH 8 AGW	56.35	0.00102
R8	S19	Saturated	pH 8 AGW	6.05	
R30	S22	Saturated	pH 8 AGW	5.15	
	J13	Unsaturated	pH 8 AGW, 1 pulse	71.0	0.00055
	J12	Unsaturated	pH 8 AGW, 2 pulse	97.8	0.0088
	J14	Unsaturated	Anionic surf., 1 pulse	70.05	0.00055
	J11	Unsaturated	Anionic surf., 2 pulse	116.1	0.00065
	J19	Unsaturated	Cationic surf. 1 pulse	129.8	0.00127
	J20	Unsaturated	Full reductant (CPS)	129.5	0.0110
	J21	2D unsaturated	pH 8 AGW 1 pulse	189.1	0.0359
	J22	2D unsaturated	Cationic surf. 1 pulse	334.6	0.458
R5	S2	Saturated	pH 8 AGW	5.61	
	S12	Saturated	pH 6 AGW	5.14	

[1]v = initial interstitial velocity (constant for water-saturated experiments).
[2]v = final interstitial velocity during residual draining of infiltration experiment.
[3]0.03 mol/L Na-dithionite +0.12 mol/L K_2CO_3 injected at 1.0 to 2.5 pore volumes only.
[4]0.03 mol/L Na-dithionite +0.12 mol/L K_2CO_3 injected for all 10 pore volumes.

Cr is usually released from dissolution of calcite, Fe oxides, and potentially other phases, so longer SF durations were applied (Qafoku et al. 2009; Szecsody et al. 2019). Changes in contaminant effluent concentration before and after the SF and the length of the SF events were used to calculate the Cr rates from the sediments (expressed in µg contaminant/g of sediment/day). Sequential extractions were also used on the pre- and postleach sediments to obtain mass balance on the Cr in the sediment.

1- and 2D Hydraulically Unsaturated Column Experiments

1D unsaturated column experiments were used to measure Cr leaching under conditions that better represent those expected during field-scale soil flushing (Table 4). These experiments consisted of infiltration of AGW or other liquid amendments into a 9.5- to 10-feet (2.9- to 3.3-m) high by 1-inch inner diameter column filled with Cr-contaminated and uncontaminated Hanford formation sediments (Figure S1). Characterization studies have shown that at field scale, Cr contamination typically occurs at a specific depth interval and the remainder of the 80- to 100-feet-deep vadose zone is not Cr contaminated (Qafoku et al. 2011). To approximate these conditions, the lowest 1.0 foot of the sediment column was packed with Cr-contaminated sediment and the remaining 8.5 to 9 feet of the column was filled with uncontaminated sediment. Because the grain size distribution of most Hanford formation sediments at field scale consisted of sandy gravel or gravely sand (with some silt), sediments used in these unsaturated leach experiments were modified to include the gravel fraction. The uncontaminated Hanford formation sediment used in all experiments consisted of 44% gravel (2 to 12 mm), 39% sand, and 17% silt/clay from the Pasco gravel pit. The Cr-contaminated sediments consisted of selected less than 2-mm sediments with 50% peak gravel added by weight. The upper size limit of the gravel added was 12 mm to fit in the 25-mm inner diameter clear PVC columns. Sediments had an initial 4% (g/g) AGW content, which is an average field water content. The bottom of the sediment column contains a 30-µm woven nylon screen, a layer of coarse #16 sand, and a layer of #30 fine sand (Accusand, Utica, I) next to the Cr-contaminated sediment. The sand layers enable water to drip out of the bottom of the column into a fraction collector.

The 1D unsaturated column experiments consisted of dripping AGW (or other amendments) at the top of the column (flow rate of 0.1 to 1.5 mL/min) using a high-performance

liquid chromatography (HPLC) pump (Figure S1, blue HPLC pumps in upper left) for 5 to 50 h, and drip collection of water samples at the bottom of the sediment column was conducted for 100 to 600 h. The interstitial velocities ranged from 4.5 to 130 cm/h (Table 4), in comparison to calculated velocities ranging from 0.7 to 102 cm/h for recent field-scale soil flushing in the Hanford 100-K West Area (DOE/RL-2019-77 2020). The flow rate was calculated from the weight of each sample and time of sampling. Sample times ranged from 4 min (for high infiltration rates of 1.0 mL/min) to 2500 min after hundreds of hours of residual water dripping out of the column, as shown by the interstitial velocity change for these infiltration experiments (Table 4). Early 1D experiments had a fraction collector mounted in a vacuum chamber, and there was a porous plate with a 1-bar air entry value at the bottom of the column (Figure S1). Although liquid samples were collected by maintaining 0.5 bars of suction for the fraction collector chamber, the flow rate through the porous plate was too slow for the 1.0-mL/min infiltration rate, so collection of samples for the remaining tests was done by gravity dripping. The Cr concentration in effluent samples was measured by inductively coupled plasma-optical emission spectrometry (ICP-OES). After all effluent samples were collected from the infiltration experiment, the column was sectioned and 10 samples were taken at differing depths to measure the final water content. Sequential extractions were also conducted on the postleach Cr-contaminated sediment to obtain mass balance on the Cr phases remaining in the sediment. Standard deviation of leached Cr in duplicate unsaturated experiments (53%) was greater than water-saturated experiments (12%) and included experiment pairs: (1) J7 and J4 (AGW at 5.26 and 10.05 cm/h, Table 4), (2) J12 and J13 (first 300 h), and (3) J11 and J14 (first 300 h).

Given the change in volumetric flow rate of water at the bottom of the infiltration column over time and the Cr concentration, the Cr flux rate ($\mu g\,Cr\,h^{-1}\,cm^{-2}$) was calculated. This is the scalable Cr flux to GW at field scale. Although this 10-feet-high column showed residual water leaching for hundreds of hours, it is likely that field-scale soil leaching with 80 to 100 feet of vadose zone would take considerably longer. Overall, the fraction of leached Cr mass as a function of PV, and Cr flux rate to groundwater from these laboratory experiments over a range of conditions, provide a technical basis for field-scale infiltration rate, number of PVs to flush, number of flush cycles, and termination of the soil flushing and P&T operations.

Extraction and Leach Sample Analyses

The Cr concentrations in the liquid sequential extractions and the water-saturated and unsaturated leach experiments were analyzed after 0.45-µm filtering for total Cr by ICP-OES with a detection limit of 0.2 µg/L (undiluted). For some amendments such as the Na-dithionite or Ca-polysulfide solution, dilution was necessary, so the detection limit was higher. A few other metals (Ba, Ca) were also analyzed in some extractions and leach experiments, as these metals complex with Cr in precipitates. The Br^- tracer in the leach experiments was quantified with ion chromatography (IC), with a detection limit of 0.1 mg/L. Other anions, such as sulfate (SO_4^{2-}) and nitrate (NO_3^-), were also quantified by IC, particularly for leach experiments containing elevated SO_4^{2-} and NO_3^- concentrations.

Simulation of 1D Infiltration Experiments

Selected 10-feet-high 1D infiltration experiments were simulated with an advection-dispersion model to obtain parameters that could be used to simulate field-scale leach solution infiltration (i.e., 80-feet vadose zone and longer time scales). As Cr was present in sediments in multiple surface phases, including aqueous pore water, adsorbed Cr, and in one or more precipitates, a model that assumes equilibrium Cr sorption or kinetic first order reversible sorption was insufficient to describe the observed dynamic leaching. However, a model used contained a kinetic reversible sorption of Cr, and in addition, a log-normal distribution of mass transfer rates (Culver et al. 1997) incorporates a range of Cr release rates and can describe most of the observed behavior. The partial differential equations that describe 1D advective transport with this model:

$$\frac{\partial C}{\partial t} = D\frac{\partial^2 C}{\partial x^2} - v\frac{\partial C}{\partial x} - \sum_{k=1}^{\mathrm{NK}} \frac{\rho \alpha_k}{\theta}\left(fK_D C - S_k\right), \quad (1)$$

$$\frac{\partial S}{\partial t} = \sum_{k=1}^{\mathrm{NK}} \alpha_k\left(fK_D C - S_k\right), \quad (2)$$

$$p(\alpha) = \frac{1}{\sqrt{2\pi}\sigma\alpha}\exp\left(-\frac{1}{2\sigma^2}(\ln(\alpha)-\mu)^2\right), \quad (3)$$

describe the change in aqueous concentration (C, µg/L) and sorbed concentration (S, µg/g) from advection (v = velocity, cm/h), dispersion (cm^2/h), and slow mass transfer defined as a long-normal probability distribution ($p(\alpha)$), where α is the rate (1/h). The probability function has a mean of the log-normal rate distribution (µ in h^{-1}) and standard deviation (σ). This type of model was previously used to describe uranium transport in Hanford sediments with a similar distribution of processes (i.e., aqueous U, adsorbed U, and U present in multiple precipitates; Qafoku et al. 2005; Bai et al. 2009).

Results and Discussion

Sediment Cr Contamination Characterization via Sequential Extractions

The changes in Cr mass associated with different solid phases of vadose and saturated zone sediments were determined using data from preleach sequential liquid extractions, column leached mass, and postleach sequential extractions; the data are summarized in Table 5. The results of these extractions are discussed in detail in the following sections of this paper.

Hydraulically Saturated Column Experiments

Most sediments showed the Cr maximum peak concentration (and bulk of mass) released within the first PV. Sediments with Cr that was quickly released (e.g., aqueous, adsorbed, and Cr in high-solubility precipitates, such as $CaCrO_4$, Table 5) showed little additional Cr released

Table 5

Cr Sequential Extractions Pre- and Postleach and Cr Leached Mass

Sediment	Experiment Before Extraction	Extraction 1 aqueous (µg/g)	Extraction 2 adsorbed (µg/g)	Extraction 3 rind carbonate (µg/g)	Extraction 4 carbonate (µg/g)	Extraction 5 Fe oxide (µg/g)	Extraction 6 hard to extract (µg/g)	Total (µg/g)	Extractions. 1-3 labile Cr (µg/g)	Leached (µg/g)
R28	None	0.0093	0.0135	0.0532	8.150	1.41	214.7	224.3	0.0760	
	None	0.0070	0.0133	0.0336	7.907	1.73	219.1	228.7	0.0539	
	S18 pH 8 saturated leach	0.149	0.0250	0.139	2.872	3.67	215.2	222.0	0.314	0.0373
	J4 pH 8 unsaturated leach	0.108	0.0288	0.150	6.846	2.15	272.7	282.0	0.286	0.0331
	J6 pH 8 unsaturated leach	0.118	0.0252	0.127	2.159	2.58	178.3	183.3	0.270	0.0238
	J7 pH 8 unsaturated leach	0.168	0.0310	0.175	2.894	6.66	198.2	208.1	0.374	0.0338
	J8 pH 8 unsaturated leach	0.204	0.0286	0.184	2.025	8.15	231.8	242.4	0.416	0.0301
	J9 red. unsaturated leach	0.0118	0.0252	0.0599	6.17	1.41	175.9	183.5	0.0969	0.0050
	J10 surf. unsaturated leach	0.0195	0.0201	0.0455	4.92	4.98	143.0	153.0	0.0851	0.0400
R25	None	0.240	0.509	0.845	5.41	4.38	31.73	43.11	1.594	
	S11 pH 8 saturated leach	0.00659	0.0187	0.157	3.79	1.084	26.47	31.53	0.182	1.609
	S16 pH 6 saturated leach	0.00947	0.0192	0.195	3.79	1.135	26.38	31.53	0.224	1.565
	S17 red. saturated leach	0.0206	0.0086	0.187	5.49	1.304	24.18	31.19	0.216	1.072
	J5 pH 8 unsaturated leach	0.0316	0.0325	0.110	1.33	0.468	13.52	15.49	0.174	0.331
R8	None	0.6368	0.4802	0.2056	0.704	1.060	25.85	28.94	1.323	
	S19 pH 8 saturated leach	0.179	0.0618	0.0928	0.0730	0.343	24.64	25.39	0.3340	1.114
R5	None	0.217	1.20	0.857	2.919	1.373	11.40	17.96	2.271	
	S2 pH 8 saturated leach	0.0711	0.0518	0.134	2.26	0.553	7.31	10.38	0.257	1.395
	S12 pH 6 saturated leach	0.0430	0.0533	0.125	2.48	0.534	8.37	11.60	0.221	1.025
$CaCrO_4$	none	7081	14,730	4987	174	0.083	0.251	26,971	26,797	
R30	None	4.895	11.40	2.785	0.875	0.401	5.139	25.49	19.07	
	None	4.841	11.87	3.280	0.462	2.880	5.564	28.90	19.99	
	S22 pH 8 saturated leach	0.202	0.976	0.821	0.989	0.257	5.577	8.821	1.998	16.61
	J11 unsaturated leach	2.267	7.241	3.321	2.655		3.851	19.33	12.83	1.24
	J12 unsaturated leach	1.331	7.675	3.744	3.157		4.527	20.43	12.75	2.07
	J13 unsaturated leach	2.962	10.066	3.461	4.134		5.930	26.55	16.49	1.34
	J14 unsaturated leach	3.414	8.661	3.883	5.464		6.665	28.09	15.96	0.730
	J19 unsaturated leach	3.623	9.493	3.313	2.399		5.308	24.14	16.43	4.04
	J20 unsaturated leach	0.043	6.973	3.995	6.225		6.646	23.88	11.01	0.607

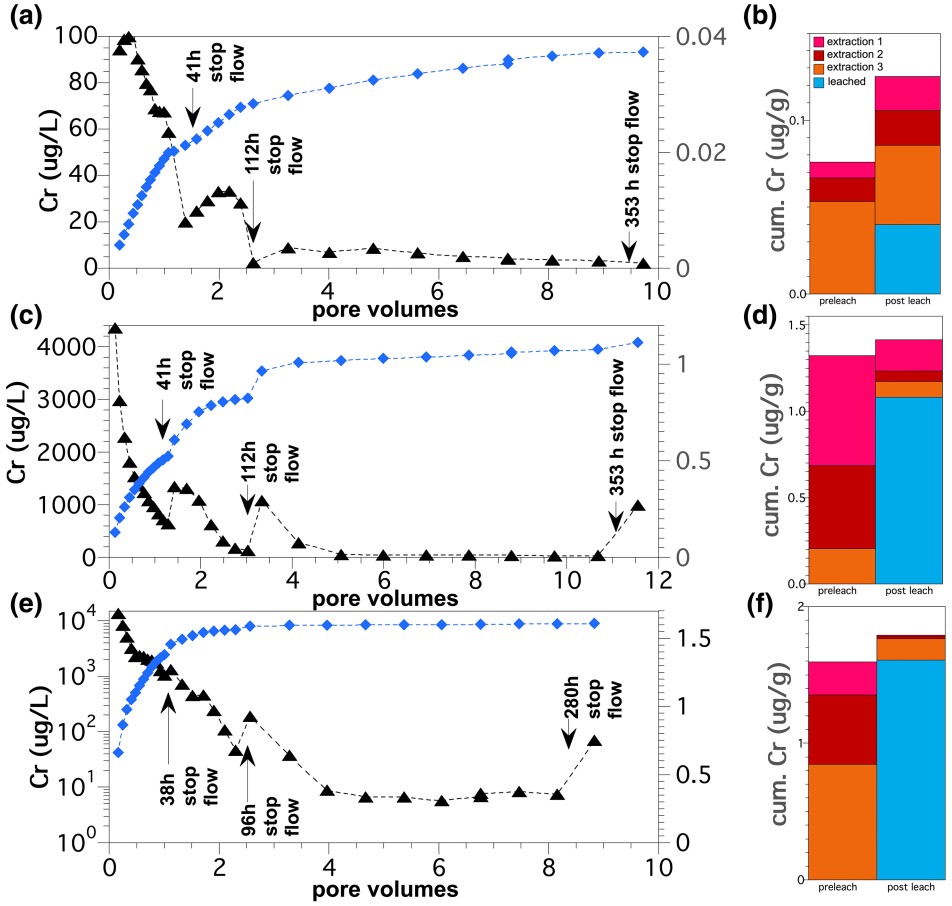

Figure 1. Cr leaching in 1D water-saturated columns (a, c, e) and corresponding pre- and postleach sequential extractions (b, d, f). Sediment R28 showed fast Cr release (a, b, exp. S18), whereas sediments R8 (c, d, exp. S19) and R25 (e, f, exp. S11) showed fast and slow Cr release. Cr concentrations in black triangles and cumulative Cr leached (µg/g) in blue diamonds.

after 2 PVs, and no increase in Cr concentration after the SF events. For one sediment, Cr leached within the first 2.5 PVs, and low or background Cr concentrations were observed from 2.5 to 10 PVs (R28, Figure 1a). Cr concentration changed little during the SF events (shown with black arrows), indicating that there is little additional Cr release from the sediment. Previous studies have shown that natural Cr in Hanford sediments exists in multiple mineral phases predominantly as Cr(III) with a small fraction (less than 5%) as Cr(VI) (DOE 1993). In contrast, anthropogenic Cr released to subsurface sediments is typically released as Cr(VI), but can precipitate as Cr(VI) or Cr(III) phases, depending on the redox environment (Qafoku et al. 2003, 2010). The Cr(VI) phases include aqueous and adsorbed Cr, $CaCrO_4$, and $BaCrO_4$ (Szecsody et al. 2019). Sediment R28 contains considerable anthropogenic Cr as $BaCrO_4$, which has a low solubility and low leaching, and a 10 PV leach removed 0.0373 µg/g Cr. A comparison of the postleach sequential extraction to preleach extractions shows little change in aqueous and adsorbed Cr, but a decrease in extraction 4, so some Cr-substituted carbonate may have dissolved (Table 5, sediment R28, and Figure 1b). Chromium leaching mass and rates were determined during continuous flow and SF events applied at different times during leaching (Table S2).

In contrast, field-contaminated sediments that had additional Cr in phases that dissolved slowly (e.g., CrO_4-substituted calcite, $BaCrO_4$) showed elevated Cr concentrations over most PVs and after SF events (sediments R8 and R25, Figure 1c and 1e). These two sediments exhibited both fast and slow Cr release, with initial peak concentrations of 4000 (sediment R8) to 10,000 µg/L (sediment R25), and both had additional high-concentration peaks after SF events. Sequential extractions performed in sediments before leaching (Table 5 and Figure 1d and 1f) showed that the first three extractions (i.e., labile Cr) for preleach sediments correlated with the mass of Cr leached within the first 10 PVs; i.e., the leached fractions (blue in Figure 1d and 1f) were similar to the total of the first three extractions.

In summary, leaching with a pH = 8 AGW solution showed that the Cr mass and rate varied by orders of magnitude in the field-contaminated Hanford sediments. Sediments with higher Cr mass released Cr at faster rates (Figure 2), likely due to the greater fraction of anthropogenic Cr mass, which was more easily removed. The Hanford sediments with high Cr mass (R8 in experiment S19, R25 in experiment S11, Table 5) released more than 1 µg/g of Cr at rates that were 1 to 5 orders of magnitude faster than sediments with low Cr mass. Sediment R30 (leach experiment S22) is a synthetic sediment composed of Hanford formation sediment with additions of $CaCrO_4$,

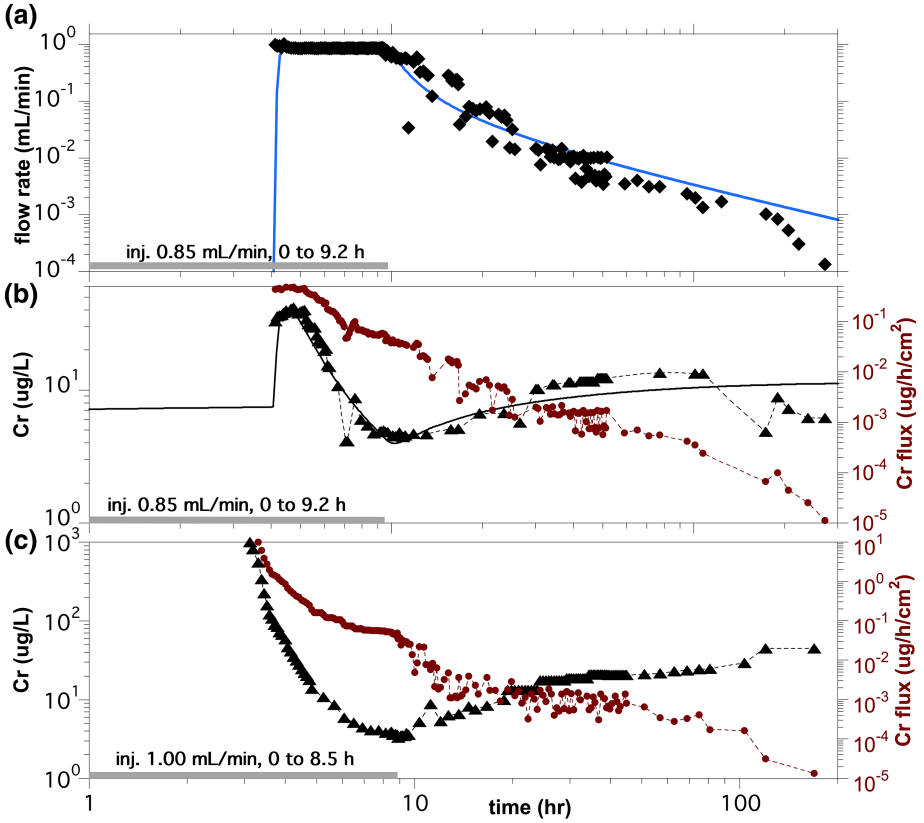

Figure 2. Chromate leaching in 10-feet high 1D infiltration columns: (a) water flux for sediment R28, experiment J6 (b) Cr concentration and flux for sediment R28, exp. J6 and (c) Cr concentration and flux for sediment R25 (exp. J5). Solid lines are simulation fit to flow and Cr concentration data.

Cr-substituted calcite, and $BaCrO_4$. Sequential extractions on $CaCrO_4$ alone showed that 26% dissolved in extraction 1 (groundwater), 55% in extraction 2 (ion exchange solution), and 18% in extraction 3 (Table 5). Extractions completely dissolved the $CaCrO_4$, yielding 26.8 mg/g Cr, compared to the calculated yield of 27.3 mg/g Cr. Sequential extractions for the synthetic sediment R30 showed that the Cr mass leached (16.6 µg/g) was close to Cr lost in the in the first three extractions by leaching (i.e., preleach extractions minus post leach extractions, 18.4 µg/g), so likely all of the $CaCrO_4$ leached, the Cr-substituted calcite and most of the $BaCrO_4$ (Cr added total 19.5 µg/g). For this artificial sediment, leaching of the $BaCrO_4$ appeared more rapid than in field sediment R28, which contained considerable $BaCrO_4$ (~190 µg/g, Table 5, extraction 6 minus natural averaging 30 µg/g). There may be additional processes that occurred in the field for the decades of $BaCrO_4$-sediment contact for sediment R28 that slowed the leaching of Cr compared to artificial addition of $BaCrO_4$ to sediment R30 which exhibited more rapid Cr leaching. Sediment R30 showed similar Cr release rates to the other field-contaminated sediment, but with greater leached mass, indirectly implying that these phases were contributing to Cr leaching from the naturally contaminated sediments.

Hydraulically Unsaturated Column Experiments

Packed column (10 feet high) experiments were used to evaluate Cr leaching behavior under unsaturated conditions. For three field sediments (R5, R25, and R28), significantly less Cr leached in unsaturated conditions (27.0 ± 22.2%) with AGW compared to water-saturated leaching (Table 5). In the experiment conducted with sediment R30, only 10% of the Cr mass was removed under unsaturated conditions compared to water-saturated conditions (Table 5). There were differences between hydraulically saturated and unsaturated column experiments, but sediment-leach water contact times were similar (i.e., ~500 h including SF events for saturated and ~430 h for unsaturated experiments). Water infiltration through unsaturated sediments is typically through larger pores, although capillary forces can move water into smaller pores, so mobile (i.e., leaching) pore water does not access all pore water; thus, even adsorbed Cr leaches more slowly due to additional diffusion time between immobile and mobile pore water. Under saturated, pressure-driven conditions, water is forced through most pores irrespective of size. Thus, leaching tends to be less efficient under unsaturated conditions as only the grain surfaces of larger pores are in contact with infiltrating water. This is a similar conclusion to those found in previous studies for leaching of Cr (Qafoku et al. 2011) and uranium (Szecsody et al. 2012a, 2012b).

Water infiltration was only constant when water was being injected at the sediment surface. For example, for infiltration experiment J6, water was injected at 0.85 mL/min for the first 8.5 h (gray bar, Figure 2a). Residual leaching occurred after the infiltration water was no lon-

Table 6

Model Parameters Used to Simulate Unsaturated Leach Experiments

Sediment	Experiment No.	Infiltration Rate (cm/h)	K_d (cm^3/g)	log μ (1/h)	log σ
R28	J6 unsaturated	47.4	0.55	−3.8	3.0
	J7 unsaturated	5.26	0.55	−5.2	3.0
	J8 unsaturated	16.5	0.60	−2.0	3.0
R30	J12 unsaturated	97.8	0.45	−5.4	1.0

ger applied (i.e., more than 8.5 h) and water leached out of the column at a progressively slower rate. The 1D reactive transport model fit the water drainage well (blue line, Figure 2a). This is representative of the water flux to GW at field scale. In infiltration experiment J6, Cr concentration was initially high, peaking at 5 h (Figure 2b, black triangles), then decreased by 10 h. However, during the residual water leaching phase (i.e., 8.5 to 300 h), as the water flux rate decreased, this resulted in higher sediment-water contact times, and the Cr concentration increased slightly, from 4 to 15 μg/L, then decreased after 100 h. Simulation of the Cr concentration was well approximated for the first 80 h, as shown by the black line in Figure 2b (model parameters in Table 6). In this 10-feet-high laboratory column, the Cr flux to GW decreased by orders of magnitude over time during the residual leaching (red circles, Figure 2b), so it is likely to be inconsequential at field scale. In contrast, for a sediment that exhibits both fast and slow Cr release (sediment R25, Figure 2c), during residual water leaching, the Cr concentration increased from 3.5 μg/L at 10 h to 43 μg/L by 200 h. In this case, the Cr flux to GW from 10 to 80 h decreased only slightly, as the increasing Cr concentration is nearly offsetting the decrease in water flux.

In unsaturated flow conditions, water advection occurs through larger pores, and water diffusion driven by capillary forces occurs in smaller pores. Because slower infiltration rates should access a greater fraction of pores, experiments at three infiltration rates were conducted using sediment R28. (Effluent samples were filtered to minimize the colloidal effect on Cr transport at faster flow rates.) A plot of the cumulative leached Cr mass for the different infiltration rates shows the systematic increase in Cr leaching at slower infiltration rates (Figure 3a) at later times (and higher volume), but somewhat inconsistent leaching initially (i.e., experiment J8 with the intermediate flow rate was leaching Cr more slowly). The leached mass was a function of the infiltration rate, with the slowest infiltration rate (experiment J7) leaching 91% and the fastest infiltration rate (experiment J6) leaching 64% of the water-saturated leached Cr mass (experiment S18, which leached 0.0373 μg/g). The results suggest that slower infiltration should be recommended at field scale. The simulated Cr release rate (μ, Table 6) was also a function of the infiltration rate, with a slower release rate for faster infiltration experiments (J7 then J8 then J6). Another experiment conducted with sediment R30 (Figure 3b) showed that injection of two 3.5-h pulses of water, separated by 300 h, leached greater Cr mass than a single 7-h injection of water at the same flow rate. In contrast to simulations with sediment R28 experiments, a simulation showed a rapid Cr release rate for experiment J12 (sediment R30). Sediment R30 contained a large fraction of high-solubility $CaCrO_4$ (likely dissolved in extractions 1 and 2, Table 5), and a small fraction of low-solubility Cr-substituted calcite (dissolved in extractions 3 and 4), and generally released most Cr rapidly (Figure 3b). For the two-pulse experiment, the first pulse leached some Cr but then left higher residual water in the unsaturated sediment for 300 h, which allowed more time for the Cr to dissolve from precipitates and partition into the pore water. This Cr was then leached out with the second infiltration pulse. This is similar to the Cr released during SF events in the water-saturated experiments ("Hydraulically unsaturated column experiments" section). In comparison, recent field-scale soil flushing at the Hanford 100-K West Area occurred through a series of four infiltration/drainage pulses with an estimated total of 2.5 PVs of water flushed through the vadose zone in the first two pulses and an estimated 2 PVs for the final two pulses (DOE/RL-2019-77 2020; SGW-67175). Additional Cr was leached with subsequent pulses, as in multiple pulse laboratory experiments.

Influence of Amendments on Cr Leaching

The hydraulically saturated and unsaturated experiments with AGW were used as a baseline for comparison of Cr leaching behavior with different amendments to the leaching solution.

Acidic Dissolution of Minerals to Induce Cr Leaching

Past research has demonstrated that Cr can be incorporated into soil minerals (e.g., calcite, Fe-oxides; Saslow et al. 2019; Katsenovich et al. 2021), but immobilized Cr may be released as minerals undergo dissolution. A previous evaluation of acid dissolution of Hanford, Cold Creek, and Ringold sediments showed that considerable calcite can be quickly dissolved, followed by the slow dissolution of other minerals present in the sediments including clays, for example, montmorillonite (Szecsody et al. 2013). To dissolve all the calcite in the Hanford or Ringold formation sediments (at a porosity of 35% and dry bulk density of 1.64 g/cm^3), a total of 825 or 600 PVs of pH = 3 water or 82,500 and 60,000 PVs of pH = 5 water is needed, based on the acid neutralization capacity (Szecsody et al. 2013). However, given that anthropogenic Cr was released within the past few decades, Cr-substituted calcite is likely distributed only near the outer surface (i.e., rind), so partial dissolution of calcite may release considerable Cr.

Therefore, to determine the effect of acid dissolution on Cr removal, saturated column experiments were conducted

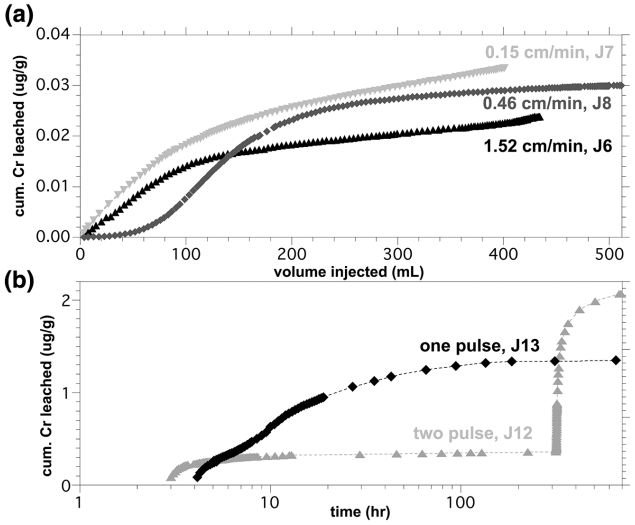

Figure 3. Influence of water application rate on Cr leached mass during unsaturated flow for: (a) different infiltration rates (sediment R28, exp. J6, J7, J8), and (b) single 7-h pulse (black, exp. J13) or two 3.5 h pulses (gray) of infiltrating water (sediment R30, exp. J12).

in which sediments were exposed to AGW (pH 8.0) or AGW that had been acidified with HNO_3 to pH 6. The results, however, showed less Cr leaching with pH 6 groundwater for sediment R5 (experiments S2, S12) and R25 (experiments S11, S16, Table 5) compared to pH 8 groundwater. Most likely, the weak acid solutions did not remove Cr from the contaminated sediments because the acid was consumed by the acid dissolution of multiple minerals in the sediments. Similar to laboratory experiments, field-scale soil flushing with pH 6 or pH 7 water showed no evidence of a pH change in the extracted groundwater, so likely no change in Cr leaching (DOE/RL-2019-77 2020). Although some of these experiments showed that weak acid solutions could be effective at increasing Cr leaching from sediments, application of these laboratory results to field scale is challenging because Cr contamination occurs at different depths within the vadose zone, and the weak acid applied to the surface will be neutralized by calcite dissolution in shallow sediments, greatly decreasing efficiency. If the weak acid solutions could be applied at depth near the Cr-contaminated sediment, Cr leaching would likely be increased.

Surfactant Application to Increase Diffusive Controlled Cr Leaching

At field scale, low-permeability inclusions exhibit slower water advection or are partially or fully bypassed by advective water flow during leaching. In addition, low-permeability inclusions generally have a higher water content and greater reactive surface area of the finer-grained materials and so may contain greater aqueous, adsorbed, and precipitated Cr. While soil flushing with groundwater may partially or fully bypass low-permeability inclusions, the presence of a surfactant in the leach water will decrease the water surface tension, which leads to somewhat greater flow in these low-permeability inclusions.

To study the effect of surfactants on Cr leaching, unsaturated 1D and 2D column experiments were conducted in

Table 7

Change in Chromate Leach Mass with the Addition of a Surfactant

Sediment	Experiment No.	Solution	Leached (µg/g)
R28	S18 saturated	pH 8 AGW	0.0373
	J6 unsaturated	pH 8 AGW	0.0238
	J10 unsaturated	Anionic Surfactant	0.0400
	J13 unsaturated	pH 8 AGW, 1 pulse	1.338
R30	J12 unsaturated	pH 8 AGW, 2 pulse	2.067
	J14 unsaturated	Anionic surf. 1 pulse	0.730
	J11 unsaturated	Anionic Surf. 2 pulse	1.24
	J19 unsaturated	Cationic Surf. 1 pulse	4.041

which sediments were exposed to AGW (pH 8) without surfactant and AGW with anionic (Na lauryl sulfate, Williams et al. 1955) or cationic (benzalkonium-Cl) surfactants. 1D infiltration with an anionic surfactant increased Cr leaching for one sediment (R28, experiment J10, Table 7) but slightly decreased Cr leaching for a second sediment (R30, experiments J14 and J11, Table 7). In contrast, 1D infiltration with a cationic surfactant greatly increased Cr leaching (experiment J19, Table 7 and Figure 4) relative to pH 8 AGW (experiment J13). A 2D flow experiment was conducted with the infiltration of AGW or AGW with a cationic surfactant into a sediment containing Cr-contaminated inclusions (Figure 5). This qualitative comparison of GW infiltration in the absence (Figure 5, left) and presence (Figure 5, right) of the cationic surfactant clearly demonstrated the role of the cationic surfactant in penetrating the low-permeability inclusions. Comparing Cr flux rate to groundwater without and with surfactants showed that the cationic surfactant resulted in greater Cr flux over the short and long term (red triangles, Figure 6), whereas the anionic surfactant resulted in less Cr flux over the short term (purple triangles) compared to groundwater leaching (black circles), and the Cr flux approached that for groundwater over the long term.

Reductant Applications to Decrease Residual Cr Leaching

For sediments that exhibit slow and fast Cr release, water-saturated leach experiments show additional Cr released during SF events at higher PVs (i.e., Figure 1c and 1e), and during unsaturated leaching, the pore water concentration increases considerably during residual water flow (i.e., Figure 2c). The persistent Cr flux from the vadose zone to groundwater is observed at the Hanford Site in some areas (DOE/RL-2019-77 2020; DOE/RL-2021-31 2022), indicating the need for additional vadose treatment by excavation or soil flushing. As a large number of soil flushing PVs would be needed for these sediments that exhibit slow Cr release, the use of an aqueous reductant was investigated to decrease the Cr leaching during the residual water flow (i.e., drainage) phase of soil flushing. For these experiments, saturated and unsaturated 1D column experiments were conducted with AGW and AGW with Na-dithionite or Ca-polysulfide on sediments that

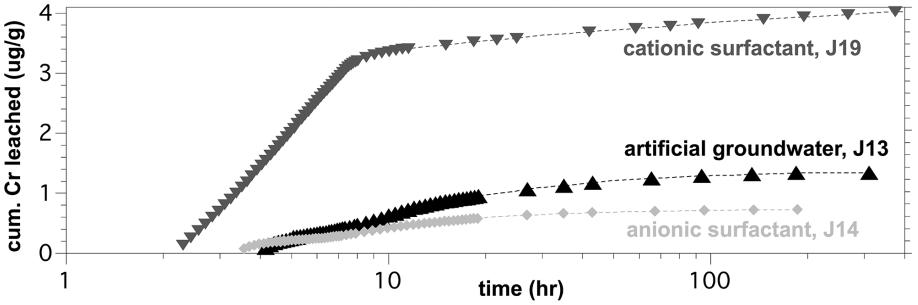

Figure 4. Influence of addition of a cationic or anionic surfactant to increase Cr leaching for sediment R30 (AGW exp. J13, anionic surfactant exp. J14, cationic surfactant exp. J19).

Figure 5. Qualitative comparison of groundwater infiltration (left side) showing predominantly flow around the low permeability inclusion or an anionic surfactant (right side) showing flow through and around the low permeability inclusion. Groundwater infiltration at top left green dot and surfactant infiltration at top right red dot.

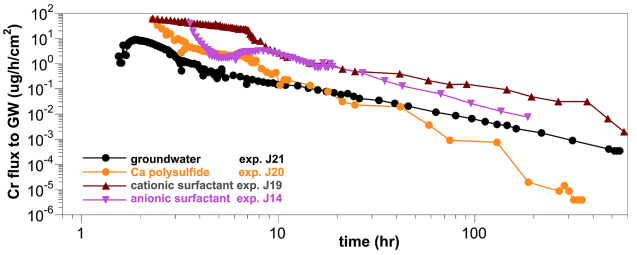

Figure 6. Unsaturated chromium leaching in 1D/2D infiltration experiments in different solutions or application sequence as shown by Cr flux to groundwater (experiments J14, J19, J20, and J21).

exhibited slow Cr release. The sediments exposed to aqueous reductants showed a significant decrease in leached Cr under both saturated and unsaturated conditions (Table 8 and Figure 7). Previous studies have shown that these reductants reduce aqueous $Cr(VI)O_4^{2-}$ to solid chromium hydroxide phases, $Cr(III)(OH)_3$ or $(Cr, Fe)(OH)_3$ (Eary and Rai 1988; Loyaux-Lawniczak et al. 2000). In unsaturated conditions during residual water flow, the calculated Cr flux to groundwater was 2 to 3 orders of magnitude less with a reductant (Ca-polysulfide, orange circles, Figure 6) compared to groundwater leaching (black circles, Figure 6). Negative release rates during SF (Table S2) indicated net Cr uptake during the SF event, possibly from the reduction of Cr(VI) to precipitate $Cr(III)(OH)_3$. However, the Cr mass removed decreased to 79% of the total Cr mass when the reductant was added in unsaturated conditions, which was less than the 93% Cr mass removed when the reductant was added in water-saturated conditions for all 10 PVs. This is most likely because some of the reductant was consumed by the oxygen present in the soil gas phase under unsaturated conditions. Infiltration of the AGW with reductant through tens of feet of unsaturated sediment over days to weeks will be even less efficient than the 10-feet infiltration experiment conducted here, as the reductant used (i.e., Na-dithionite) hydrolyzes with a half-life of 27 h (Szecsody et al. 2004), but infiltration of the slow-reacting reductant (Ca-polysulfide) would show greater efficiency.

Cr Mass and Release Rate

Water-saturated experiments showed a correlation between the leached Cr mass and the Cr release rate, as calculated from SF events (Figure 8). Sediments with low labile Cr (i.e., extractions 1, 2, and 3) released the small amount of Cr quickly but the release rate was small (Figure 8, points grouped in rectangle). In contrast, sediments with high leached Cr mass (e.g., sediments R8, R25 and others) exhibited more complex behavior as Cr was present in multiple phases, which resulted in the bulk of Cr releasing quickly and the rest continuing to leach for many PVs with a slower release rate at high PVs (sediments on the right side of Figure 8). Although only 10 to 12 PVs were leached through the column in this study, Szecsody et al. (2019) demonstrated that this type of sediment showed slow Cr release even when it was leached for 100 PVs, and after SF events.

Table 8

Change in Chromate Leach Mass with the Addition of a Reductant

Sediment	Experiment	Solution	Leached (µg/g)
R25	S11 saturated	pH 8 groundwater	1.61
	S17 saturated	Part reductant (dithionite)	1.072
R28	J6 unsaturated	pH 8 groundwater	0.0238
	J9 unsaturated	Full reductant (dithionite)	0.0050
R30	J13 unsaturated	pH 8 groundwater	1.338
	J20 unsaturated	Full reductant (Ca polysulfide)	0.607

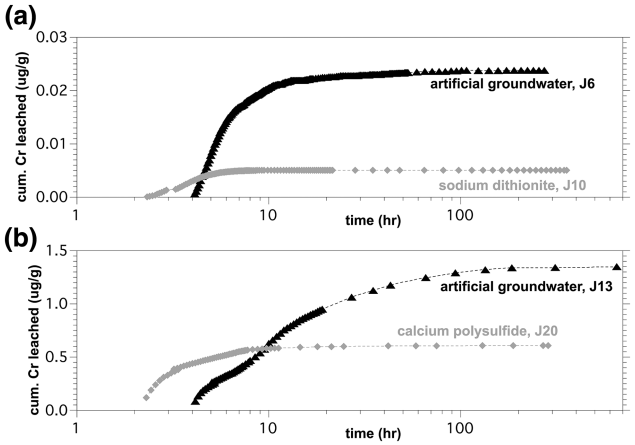

Figure 7. Influence of a reductant to decrease Cr leaching during residual water movement after unsaturated water infiltration for: (a) Na-dithionite (sediment R28, exp. J6 and J10), and (b) Ca-polysulfide (sediment R30, exp. J13 and J20).

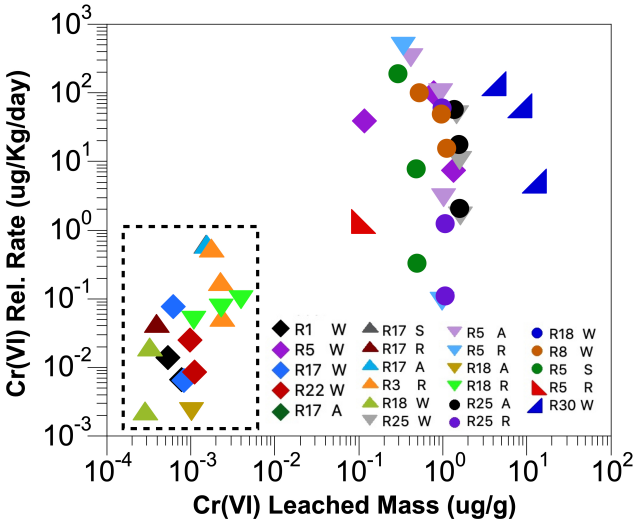

Figure 8. Chromate leached mass and release rate for sediments leached with artificial groundwater. For each sediment, the leach water is: pH 8 artificial groundwater (W), pH 5 or 6 artificial groundwater (A), anionic surfactant (S), or sodium dithionite reductant (R).

Other than aqueous and adsorbed Cr, which leaches quickly, significant natural Cr is present in Hanford sediments (i.e., average 18.5 µg/g, range 2.9 to 33.2 µg/g; DOE 1993) incorporated as Cr(III) in mafic minerals that have very low solubility and are not susceptible to leaching. In contrast, anthropogenic Cr released to the subsurface precipitates in high- and low-solubility phases, as previously described (Qafoku et al. 2009; Szecsody et al. 2019). Therefore, the leached Cr is not correlated to the total Cr in the sediment, but the labile Cr (i.e., extractions 1, 2, and 3) is well correlated with the leached Cr for the sediments (Figure 1b, 1d, and 1f) and for other sediments (Figure 9a), as shown in sequential extractions. The release rate generally decreased between SF events at 1, 2.5, and 10 PVs (Table S2) because the release rate at 1 PV is likely due to Cr desorption whereas the Cr release rate at higher PVs is likely due to partial dissolution of progressively lower solubility Cr phases. As such, there were general trends of the Cr release rate at 1, 2.5, and 10 PVs (Figure 9b), which could be used to approximate behavior for other sediments, given the labile Cr. For sediments leached with AGW (pH 8), the initial Cr release rates at 1.0 PV were high and correlated well with adsorbed Cr mass (R^2 = 0.81, Figure 9b, red diamonds), but not with the total Cr. The Cr release rates at 2.5 PVs, in all cases, were approximately half those at 1.0 PV. These rates were somewhat correlated with adsorbed Cr mass (i.e., R^2 = 0.64, Figure 9b, blue circles). The release rates at 10 PVs were about 10 times smaller than those at 1 PV and were moderately correlated with the adsorbed Cr mass (R^2 = 0.72, Figure 9b, black triangles). Some Cr release rates, particularly at 10 PVs, were negative, most likely indicating Cr precipitation or incorporation. Fast initial rates and subsequent slow (or negative) release rates indicate that nearly all the mobile Cr has been leached. This was generally the case for sediments that had low leachable Cr and fast Cr release.

Conclusions

This study was conducted to characterize site-specific Cr release mass and rates from field-contaminated sediments and evaluate the influence of different soil flushing strategies and amendment additions on the efficiency of unsaturated soil flushing. Field-scale soil flushing can be more efficiently conducted when based on a robust technical understanding of site-specific, key geochemical and physical reactions and processes that control the moblility of aqueous and adsorbed Cr(VI), and the behavior of the Cr fraction incorporated into sediments' solid phases. This study demonstrated that the technical information needed includes the: (1) sediment Cr mass and release rate, which strongly controls the soil flushing volume and time needed to mobilize most Cr from homogeneous sediments; (2) effect on Cr leaching by application of different flushing strategies or amendment additions; and (3) effect on residual Cr leaching by reductive amendment additions after soil flushing ends.

Results of this study showed that quantifying Cr leach mass and removal rate from contaminated sediments can be used to develop an efficient field-scale Cr removal/flushing approach (along with additional field scale information such

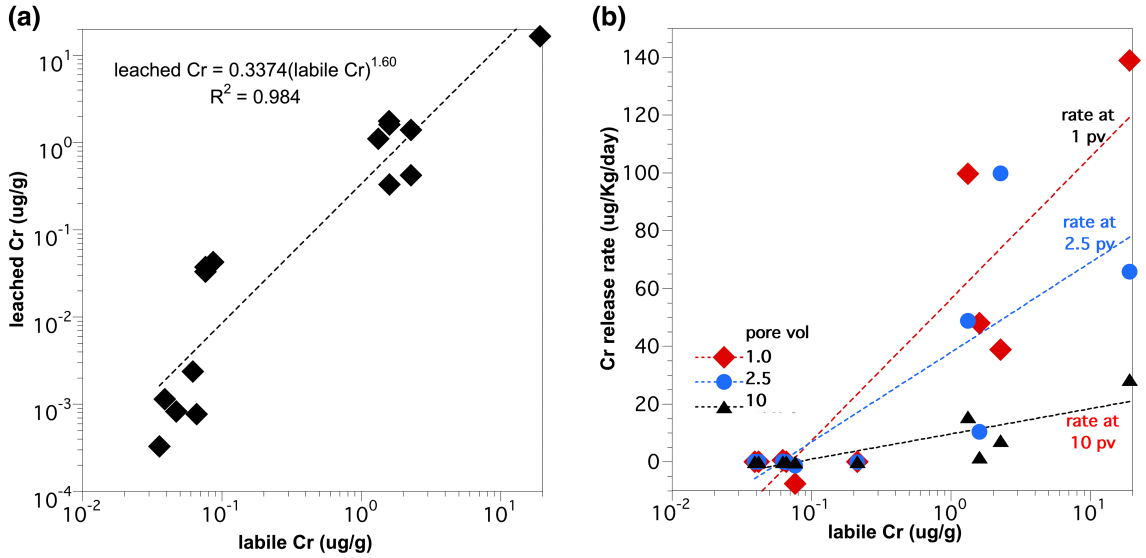

Figure 9. Relationship between (a) labile Cr and leached Cr and (b) labile Cr and Cr release rate at different pore volumes during leaching.

as permeability in the sediment profile and location of Cr contamination). The labile Cr mass (i.e., sequential extractions 1, 2, and 3) correlated well with the Cr mass leached in the column experiments, suggesting that extractions may provide an estimate of leachable Cr mass and rate under field conditions. The water-saturated column experiments showed that sediments that had low concentrations (i.e., less than 0.1 µg/g) of easily released Cr (i.e., aqueous, adsorbed, and Cr in high-solubility precipitates such as $CaCrO_4$) leached most of the Cr (i.e., more than 95%) within 3 PVs. Leaching under unsaturated conditions was less efficient (i.e., 21 to 64% Cr leached for the same PV), so more leaching (10 PVs or more) was needed to leach most of the Cr in laboratory experiments. At field scale, if low-permeability zones are present and contain Cr, additional leach PVs would be needed (dependent on multiple factors including permeability of the zones, volume, water content, and Cr phases), but enhanced Cr leaching in some cases can be achieved with the use of a surfactant. These sediments had moderate amounts of low-solubility Cr-containing precipitates (10 to 40 µg/g) that were not leachable, resulting in little additional release at later times or during SF. In contrast, sediments that had moderate to high Cr concentrations with varying aqueous and adsorbed Cr (less than 0.5 µg/g) that was readily released, and additional Cr in slowly dissolving phases (e.g., CrO_4^{2-} -substituted calcite and $BaCrO_4$), showed elevated Cr concentrations for the duration of the experiments. These sediments exhibited a range of Cr release behavior. A sediment with high-solubility Ca-chromate released 82% of the Cr by 3 PVs, whereas a sediment with Cr-substituted calcite released 12% of the Cr by 3 PVs (and 33% by 10 PVs).

A single water flush of about 10 PVs applied at a slow infiltration rate could be used to remove Cr from homogeneous sediments with low concentrations of labile, highly leachable Cr (i.e., less than 0.2 µg/g). Altering the water application rate and use of multiple pulses could be a good strategy to remove Cr from sediments with moderate to high labile Cr that is associated with a variety of Cr-bearing phases serving as a slow-releasing, long-term Cr source. For these sediments, greater Cr mass was leached when the infiltration rate was reduced by an order of magnitude and two leach pulses were used instead of one. These results provide a technical basis for using multiple soil flushing pulses at field scale; namely, after fast-release Cr is removed using the first leach pulse, the increased moisture content in the pore water and time between pulses results in additional Cr release from sediments, which is flushed in subsequent pulses. If the Cr release rate from sediments is quantified, then the wait times between flushing cycles can be quantified.

Laboratory-scale experiments also showed that adding amendments to the leach solution to increase or decrease Cr removal from the sediments demonstrated that:

1. Weak acid solutions were marginally effective and did not significantly increase Cr removal.
2. In sediments containing Cr-contaminated low-permeability lenses, the surfactant removed Cr more quickly out of the lenses due to the decrease in water surface tension, which increased water flow through lenses. A cationic surfactant was more efficient at removing Cr than an anionic surfactant.
3. The use of a fast-reacting reductant (e.g., Na-dithionite) was highly effective at decreasing residual Cr leaching after flushing had ended. In contrast, the use of a slow-reacting reductant (e.g., Ca-polysulfide) during unsaturated leaching did not decrease initial Cr leaching during fluid application, but significantly decreased Cr leaching during residual water flow. Infiltration of either reductant would likely be inefficient at field scale as it would oxidize in the vadose zone before contact with Cr-contaminated sediments, but the slow-reactant reductant (Ca-polysulfide) would likely infiltrate deeper. However, for sites that appear to have slow-release Cr trapped in sediments near the water table, a reductant could be added to the aquifer to decrease residual Cr leaching with little loss due to oxidation.

In general, knowledge of the Cr release mass and rate from contaminated sediments can be used to improve field-scale soil flushing operations. This does require sediment samples, but laboratory leach studies can more effectively quantify the mass of leachable Cr and release rate, which can indicate which sites would be more efficiently leached with multiple infiltration pulses and the addition of a surfactant and which sites would likely require the use of a reductant to decrease residual Cr leaching into groundwater.

Acknowledgments

This document was prepared by the Deep Vadose Zone—Applied Field Research Initiative at Pacific Northwest National Laboratory. Funding for this work was provided by the U.S. Department of Energy (DOE) Richland Operations Office. The Pacific Northwest National Laboratory is operated by Battelle Memorial Institute for the DOE under Contract DE-AC05-76RL01830. The authors would like to thank internal reviewers for comments that significantly improved the manuscript.

Supporting Information

Additional supporting information may be found online in the Supporting Information section at the end of the article.

Table S1. The chemical composition of the artificial groundwater used in extraction 1 and in the column experiments.

Table S2. Cr release rate change during hydraulically saturated leaching calculated from stop flow.

Figure S1. 10-feet-high 1D infiltration columns with effluent at bottom leading into fraction collectors located in vacuum chambers (bottom left), and enlargement of the bottom of the column showing infiltration front (right).

References

Arcon, I., B. Mirtic, and A. Kodre. 2005. Determination of valance states of chromium in calcium chromates using X-ray adsorption near-edge structure (XANES) spectroscopy. *Journal of the American Ceramic Society* 81, no. 1: 222–224.

Bai, J., C. Liu, and W. Ball. 2009. Study of sorption-retarded U(VI) diffusion in Hanford silt/clay material. *Environmental Science & Technology* 43, no. 20: 7706–7711.

Brodie, E., D. Joyner, B. Faybishenko, M. Conrad, C. Rios-Valazquez, J. Malave, R. Martinez, B. Mork, A. Willett, S. Koenigsberg, et al. 2011. Microbial community response to addition of polylactate compounds to stimulate hexavalent chromium reduction in groundwater. *Chemosphere* 85, no. 4: 660–665.

Chao, T., and L. Zhou. 1983. Extraction techniques for selective dissolution of amorphous iron oxides from soils and sediments. *Soil Science Society of America Journal* 47, no. 2: 225–232.

Culver, T., S. Hallisey, D. Sahoo, J. Deitsch, and J. Smith. 1997. Modeling the desorption of organic contaminants from long-term contaminated soil using distributed mass transfer rates. *Environmental Science & Technology* 31, no. 6: 1581–1588.

DOE. 1993. *Hanford Site Background: Part 1, Soil Background for Nonradioactive Analytes*. DOE/RL-92-94, Rev. 1, UC-630, 721, p. 243. Richland, Washington: U.S. Department of Energy, Richland Operations Office.

DOE/RL-2019-77. 2020. *KW Soil Flushing Treatability Test Report. Rev. 0*. Richland, Washington: U.S. Department of Energy, Richland Operations Office.

DOE/RL-2021-31. 2022. *183.1KE Headhouse Soil Flushing Sampling and Analysis Plan. Rev. 0*. Richland, Washington: U.S. Department of Energy, Richland Operations Office.

Dong, H., R.K. Kukkadapu, J.K. Fredrickson, J.M. Zachara, D.W. Kennedy, and H.M. Kostandarithes. 2003. Microbial reduction of structural Fe(III) in illite and goethite. *Environmental Science & Technology* 37: 1268–1276.

Dresel, P.E., N.P. Qafoku, J.P. McKinley, J.S. Fruchter, C.C. Ainsworth, C. Liu, E.S. Ilton, and J.L. Phillips. 2008. *Geochemical Characterization of Chromate Contamination in the 100 Area Vadose Zone at the Hanford Site*. PNNL-17674. Richland, Washington: Pacific Northwest National Laboratory.

Eary, L.E., and D. Rai. 1988. Chromate removal from aqueous wastes by reduction with ferrous iron. *Environmental Science & Technology* 22, no. 8: 972–977.

Gleyzes, C., S. Tellier, and M. Astruc. 2002. Fractionation studies of trace elements in contaminated soils and sediments: A review of sequential extraction procedures. *Trends in Analytical Chemistry* 21, no. 6 & 7: 451–467.

Hall, G., J. Vaive, R. Beer, and N. Hoashi. 1996. Selective leaches revisited, with emphasis on the amorphous Fe oxyhydroxide phase extraction. *Journal of Geochemical Exploration* 56: 59–78.

Jacobs, J., and S. Testa. 2005. Overview of chromium(VI) in the environment: Background and history. In *Chromium(VI) Handbook*, ed. J. Guertin, J. Jacobs, and C. Avakian, 1–21. Boca Raton, Florida: CRC Press.

Katsenovich, Y., R.T. Gort, R. Gudavalli, J. Szecsody, V.L. Freedman, and N.P. Qafoku. 2021. Silicon concentration and pH controls over competitive or simultaneous incorporation of iodate and chromate into calcium carbonate phases. *Applied Geochemistry* 128: 104941.

Larner, B., A. Seen, and A. Townsend. 2006. Comparative study of optimized BCR sequential extraction scheme and acid leaching of elements in certified reference material NIST 2711. *Analytica Chimica Acta* 556: 444–449.

Last, G.V., M.M.V. Snyder, W. Um, J.R. Stephenson II, C.E.S. Leavy, D.H. Bacon, N.P. Qafoku, and R.J. Serne. 2015. *Technetium, Iodine, and Chromium Adsorption/Desorption Kd Values for Vadose Zone Pore Water, ILAW Glass, and Cast Stone Leachates Contacting an IDF Sand Sequence*. PNNL-24683. Richland, Washington: Pacific Northwest National Laboratory.

Loyaux-Lawniczak, S., P. Refait, J. Ehrhardt, P. Lacomte, and J. Genin. 2000. Trapping of Cr by formation of ferrihydrite during the reduction of chromate ions by Fe(II)-Fe(III) hydroxysalt green rusts. *Environmental Science & Technology* 34, no. 3: 438–443.

Mossop, K., and C. Davison. 2003. Comparison of original and modified BCR sequential extraction procedures for the fractionation of copper, iron, lead, manganese, and zinc in soils and sediments. *Analytica Chimica Acta* 478: 111–118.

Palmer, C.D., and P.R. Willbrodt. 1991. Processes affecting the remediation of chromium-contaminated sites. *Environmental Health Perspectives* 92: 25–40.

Qafoku, N.P., E.P. Dresel, J.P. Mckinley, E.S. Ilton, W. Um, C.T. Resch, R.K. Kukkadapu, and S.W. Petersen. 2011. *Geochemical Characterization of Chromate Contamination in the 100 Area Vadose Zone at the Hanford Site*. PNNL-17865. Richland, Washington: Pacific Northwest National Laboratory.

Qafoku, N.P., P.E. Dresel, E. Ilton, J.P. McKinley, and C.T. Resch. 2010. Chromium transport in an acidic waste contaminated subsurface medium: The role of reduction. *Chemosphere* 81, no. 11: 1492–1500.

Qafoku, N.P., P.E. Dresel, J.P. McKinley, C. Liu, S.M. Heald, C.C. Ainsworth, J.L. Phillips, and J.S. Fruchter. 2009. Pathways of aqueous Cr (VI) attenuation in a slightly alkaline oxic subsurface. *Environmental Science & Technology* 43, no. 4: 1071–1077.

Qafoku, N.P., J.M. Zachara, C. Liu, P.L. Gassman, O.S. Qafoku, and S.C. Smith. 2005. Kinetic desorption and sorption of U(VI) during reactive transport in a contaminated Hanford sediment. *Environmental Science & Technology* 39, no. 9: 3157–3165.

Qafoku, N.P., C.C. Ainsworth, J.E. Szecsody, O.S. Qafoku, and S.M. Heald. 2003. Effect of coupled dissolution and redox reactions on Cr(VI)aq attenuation during transport in the sediments under hyperalkaline conditions. *Environmental Science & Technology* 37: 3640–3646.

Rai, D., L. Eary, and J. Zachara. 1989. Environmental chemistry of chromium. *Science of the Total Environment* 86, no. 1: 15–23.

Robles-Camacho, J., and M.A. Armienta. 2000. Natural chromium contamination in groundwater at Leon Valley, Mexico. *Journal of Geochemical Exploration* 68, no. 3: 167–181.

Rockhold, M.L., X. Song, Z. Zhang, N.P. Qafoku, M.A. Jensen, J.L. Downs, J.D. Tagestad, et al. 2020. *Spatiotemporal Analyses of Groundwater and Shoreline Cr(VI) Concentrations in the 100 Areas at Hanford*. PNNL-30483. Richland, Washington: Pacific Northwest National Laboratory.

Saslow, S., S. Kerisit, T. Varga, K. Johnson, N. Avalos, A.E. Lawter, and N.P. Qafoku. 2019. Chromate effect on iodate incorporation into calcite. *ACS Earth and Space Chemistry* 3, no. 8: 1624–1630.

SGW-67175. 2021. *100-KR-4 183.1kW Headhouse Soil Flushing Results from January 2020 through May 2021. Rev. 0*. Richland, Washington: Central Plateau Cleanup Company.

Shams, K., G. Tichy, A. Fischer, M. Sager, T. Peer, A. Bashar, and K. Filip. 2010. Aspects of phytoremediation for chromium contaminated sites using common plants *Urica dioica*, *Brassica napus* and *Zea mays*. *Plant and Soil* 328: 175–189.

Stanin, F.T. 2005. The transport and fate of chromium(VI) in the environment. In *Chromium(VI) Handbook*, ed. J. Guertin, J. Jacobs, and C. Avakian, 165–207. Boca Raton, Florida: CRC Press.

Sutherland, R., and F. Tack. 2002. Determination of Al, Cu, Fe, Mn, Pb, and Zn in certified reference materials using the optimized BCR sequential extraction procedure. *Analytica Chimica Acta* 454: 249–257.

Szecsody, J., N. Qafoku, A. Lawter, R. Mackley, H. Emerson, and C. Resch. 2022. *Laboratory Evaluation to Increase Effectiveness of Field-Scale Soil Flushing in the Hanford 100 Areas, PNNL-31980 Rev 1*. Richland, Washington: Pacific Northwest National Laboratory.

Szecsody, J., N. Qafoku, A.R. Lawter, R.D. Mackley, H.P. Emerson, and C.T. Resch. 2021. *Laboratory Evaluation to Increase Effectiveness of Field-Scale Soil Flushing in the Hanford 100 Areas*. PNNL-31980. Richland, Washington: Pacific Northwest National Laboratory.

Szecsody, J., H. Emerson, R. Mackley, C. Resch, and S. Baum. 2020a. *Identification of Chromium Mass and Release Rate from 100-KR-4 Sediments*. PNNL-30385. Richland, Washington: Pacific Northwest National Laboratory.

Szecsody, J., C. Resch, O. Oafoku, H. Emerson, and B. Gartman. 2020b. *100-KR-4 Sediment Analysis for Identification of Chromium Surface Phases*. PNNL-28775, Rev 1.0. Richland, Washington: Pacific Northwest National Laboratory.

Szecsody, J., M. Truex, N. Qafoku, J. McKinley, K. Ivarson, and S. Di Pietro. 2019. Persistence of chromate in vadose zone and aquifer sediments in Hanford, Washington. *Science of the Total Environment* 676: 482–492.

Szecsody, J., M. Truex, N. Qafoku, D. Wellman, T. Resch, and L. Zhong. 2013. Influence of acidic and alkaline co-contaminants on uranium migration in vadose zone sediments. *Journal of Contaminant Hydrology* 151: 155–175.

Szecsody, J., L. Zhong, M. Oostrom, V. Vermeul, J. Fruchter, and M. Williams. 2012a. *Use of Polyphosphate to Decrease Uranium Leaching in Hanford 300 Area Smear Zone Sediment*. PNNL-21733. Richland, Washington: Pacific Northwest National Laboratory.

Szecsody, J., M. Williams, J. Fruchter, V. Vermeul, and D. Sklarew. 2004. In situ reduction of aquifer sediments: Enhancement of reactive iron phases and TCE Dechlorination. *Environmental Science & Technology* 38: 4656–4663.

Szecsody, J.E., M.J. Truex, L. Zhong, T.C. Johnson, N. Qafoku, M.D. Williams, and W.J. Greenwood. 2012b. Geochemical and geophysical changes during ammonia gas treatment of vadose zone sediments for uranium remediation. *Vadose Zone Journal* 11, no. 4: 1–13.

Tang, Y., E. Elzinga, Y. Lee, and R. Reeder. 2007. Coprecipitation of chromate with calcite: Batch experiments and X-ray absorption spectroscopy. *Geochimica et Cosmochimica Acta* 71: 1480–1493.

Truex, M., J. Szecsody, N. Qafoku, R. Sahajpal, L. Zhong, A. Lawter, and B. Lee. 2015. *Assessment of Hexavalent Chromium Natural Attenuation for the Hanford Site 100 Area*. PNNL-24705. Richland, Washington: Pacific Northwest National Laboratory.

Thornton, E., T. Gilmore, K. Olsen, J. Giblin, and J. Phelan. 2007. Treatment of a chromate-contaminated soil site by in situ gaseous reduction. *Groundwater Monitoring & Remediation* 27, no. 1: 56–64.

Vermeul, V.R., B.N. Bjornstad, C.J. Murray, D.R. Newcomer, M.L. Rockhold, J.E. Szecsody, M.D. Williams, and Y.L. Xie. 2004. *In Situ Redox Manipulation Permeable Reactive Barrier Emplacement: Final Report Frontier Hard Chrome Superfund Site, PNWD-3361*. Richland, Washington: Battelle-Pacific Northwest Division.

Vermeul, V.R., M.D. Williams, J.E. Szecsody, J.S. Fruchter, C.R. Cole, and J.E. Amonette. 2002. Creation of a subsurface permeable reactive barrier. In *Groundwater Remediation of Trace Metals, Radionuclides, and Nutrients, with Permeable Reactive Barriers*, ed. D. Naftz, S. Morrison, J. Davis, and C. Fuller. Cambridge, MA: Academic Press.

Wilkin, R.T., C. Su, R.G. Ford, and C.J. Paul. 2005. Chromium-removal processes during groundwater remediation by a zerovalent iron permeable reactive barrier. *Environmental Science & Technology* 39, no. 12: 4599–4605.

Williams, R., J. Phillips, and K. Mysels. 1955. The critical micelle concentration of sodium lauryl sulphate at 25C. *Transactions of the Faraday Society* 51: 728–737.

Zachara, J.M., C. Ainsworth, G. Brown, J. Catalano, J. McKinley, O. Qafoku, S. Smith, J. Szecsody, S. Traina, and J. Warner. 2004. Chromium speciation and mobility in a high-level nuclear waste vadose zone plume. *Geochimica et Cosmochimica Acta* 68: 13–30.

Zachara, J., C. Ainsworth, C. Cowan, and C. Resch. 1989. Adsorption of chromate by subsurface soil horizons. *Soil Science Society of America Journal* 53: 418–428.

Zachara, J., D. Girvin, R. Schmidt, and C. Resch. 1987. Chromate adsorption on amorphous iron oxyhydroxide in the presence of major groundwater ions. *Environmental Science & Technology* 21: 589–594.

Zheng, Y., Y. Yan, Y. Lin, H. Li, B. Jiao, Y. Shiau, and D. Li. 2020. Synergism of citric acid and zero-valent iron on Cr(VI) removal

from real contaminated soil by electrokinetic remediation. *Environmental Science and Pollution Research* 27: 5572–5583.
Zhong, L., N. Qafoku, J.E. Szecsody, P.E. Dresel, and Z.F. Zhang. 2009. Foam delivery of calcium polysulfide to vadose zone for chromium-VI immobilization: A laboratory evaluation. *Vadose Zone Journal* 8, no. 4: 976–985.

Biographical Sketches

***James E. Szecsody**, Ph.D., P.Geo., corresponding author, is a hydrogeologist at Pacific Northwest National Laboratory (PNNL), P.O. Box 999, 902 Battelle Boulevard, Richland, WA 99352; jim.szecsody@pnnl.gov*

***Hilary P. Emerson**, Ph.D., is an environmental engineer at Pacific Northwest National Laboratory (PNNL), 902 Battelle Boulevard, Richland, WA 99352*

***Amanda R. Lawter**, is a geochemist at Pacific Northwest National Laboratory (PNNL), 902 Battelle Boulevard, Richland, WA 99352*

***Charles T. Resch**, is a geochemist at Pacific Northwest National Laboratory (PNNL), 902 Battelle Boulevard, Richland, WA 99352*

***Mark L. Rockhold**, Ph.D., is a hydrology modeler at Pacific Northwest National Laboratory (PNNL), 902 Battelle Boulevard, Richland, WA 99352*

***Rob D. Mackley**, is a hydrogeologist at Pacific Northwest National Laboratory (PNNL), 902 Battelle Boulevard, Richland, WA 99352*

***Nikolla P. Qafoku**, Ph.D., is a soil chemist at Pacific Northwest National Laboratory (PNNL), 902 Battelle Boulevard, Richland, WA 99352; Department of Civil and Environment Engineering, University of Washington, Seattle, WA 98195*